Mass accommodation of H2SO4 and CH3SO3H on water-sulfuric acid solutions from 6% to 97% RH

ARTICLE *in* THE JOURNAL OF PHYSICAL CHEMISTRY A · SEPTEMBER 2005

Impact Factor: 2.69 · DOI: 10.1021/jp0510443 · Source: PubMed

1 AUTHOR:

David R. Hanson
Augsburg College
104 PUBLICATIONS **5,081** CITATIONS

Mass Accommodation of H_2SO_4 and CH_3SO_3H on Water−Sulfuric Acid Solutions from 6% to 97% RH

D. R. Hanson

Atmospheric Chemistry Division, National Center for Atmospheric Research, Boulder, Colorado 80303

Received: March 1, 2005; In Final Form: May 10, 2005

The uptake of H_2SO_4 and CH_3SO_3H onto particles composed of water and sulfuric acid was studied in a laminar flow reactor at atmospheric pressure. Their first-order gas-phase loss rate coefficients were determined using a chemical ionization mass spectrometer. Relative humidity was varied from 6% to 97% at 295−297.5 K. The mass accommodation coefficient, α, was found to be close to unity for both species. These findings show that α does not limit particle growth rates resulting from H_2SO_4 and CH_3SO_3H uptake. Diffusion coefficients in N_2 for these two species are also reported and a significant dependence upon relative humidity was seen for H_2SO_4 but not for CH_3SO_3H. Last, production of small particles was observed due to the presence of SO_2 in particle chargers. Formation of these particles can be significantly reduced by adding an OH scavenger such as propane.

Introduction

The uptake of gas-phase H_2SO_4 by atmospheric particles plays a very important role in their formation and growth and ultimately their size and abundance.[1−5] Growth rates of nascent atmospheric particles via accumulation of gas-phase H_2SO_4 depend on the value of the mass accommodation coefficient, α. Nucleation rates can depend strongly on the abundance of H_2SO_4; thus, efficient scavenging of H_2SO_4 by large particles ($\sim$100 nm diameter) can strongly influence nucleation.[51] Thus the propensity of a gas-phase H_2SO_4 molecule to be incorporated into an atmospheric aerosol particle (mass accommodation) can influence the number density, size, and composition of aerosol and thus their climate and health effects.

Methane sulfonic acid (MSA), CH_3SO_3H, is present in the gas-phase in the atmosphere,[6,7] and its uptake by atmospheric aerosol particles can contribute to their growth.[8−10] Although recent investigations of atmospheric MSA[7,11−13] suggest it is predominantly formed heterogeneously on large particles, a small amount of MSA produced in the gas phase can be a significant growth factor for the smallest particles, those that can lead to new cloud condensation nuclei.[5] Furthermore, mass accommodation of MSA is an interesting case study for the uptake of strong acids by aqueous solutions.

The uptake of H_2SO_4 onto sulfuric acid solutions[14,16] and sulfate salts[15] has been studied previously in the laboratory. Van Dingenen and Raes[14] estimated a value of $\sim$ 0.045 (+0.045/−0.022) for α by comparing a calculated [H_2SO_4] with measurements of particle growth rates in a flow reactor at 50% relative humidity (RH). At low relative humidities, values of α of 0.75 ($\pm$0.2) and 0.65 (+0.35/−0.22) were obtained in the laboratory experiments of Jefferson et al.[15] and Poschl et al.,[16] respectively. These two experiments obtained α from measured first-order loss rates determined by following gas-phase [H_2SO_4] as it was taken up onto aerosol salt particles (RH $\leq$ 11%)[15] and bulk acid solutions (RH $\leq$ 3%).[16] An uptake efficiency for H_2SO_4 of $\sim$ 0.5 has also been estimated in field studies[6,7] from calculated H_2SO_4 lifetimes and measured aerosol surface areas.

The mass accommodation coefficient for the uptake of MSA onto aqueous droplets has been reported to be $\sim$ 0.1 ($\pm$0.02) by two groups.[17,18] Both these measurements were conducted in a cylindrical flow reactor apparatus where uptake occurs on a train of fast-moving droplets aligned along its axis (the droplet train flow reactor). The results of these experiments suggest that mass accommodation for strong acids is not efficient at high relative humidities.

There is a paucity of data regarding the value of the mass accommodation coefficient for H_2SO_4 and CH_3SO_3H for typical atmospheric conditions. This paper describes experiments on the uptake of H_2SO_4 and CH_3SO_3H by particles of dilute sulfuric acid solutions for typical atmospheric relative humidities (6−97%). The value of α was determined from the measured gas-phase loss of reactant due to uptake onto $\sim$ 50−120 nm radius droplets. Sulfuric acid content ranged from 7−70 wt % and temperature was 296.2 $\pm$1.2 K.

Experiment

The uptake of gas-phase acid onto aqueous sulfuric acid particles was studied in a vertically aligned laminar flow reactor (i.d. of 5.17 cm and length of 120 cm) operated at ambient pressure ($\sim$0.8 atm). Basically, the acid's first-order loss rate coefficient was measured for uptake onto aerosol particles that were sized (after exiting the flow reactor) with a differential mobility analyzer (DMA, custom-built, similar to TSI long version 3071) and, in a separate gas-stream, counted with a condensation nucleus counter (TSI 3760). Gas-phase reactant was detected with a chemical ionization mass spectrometer (CIMS). The experimental procedure is presented in more detail in Hanson and Kosciuch.[19] Provided here are detailed descriptions of modifications to the experimental apparatus and procedures such as reactant sources and the chemical ionization schemes used for detection of the gas-phase acid.

Reactant CH_3SO_3H was introduced through a moveable injector by a small flow, 30−70 sccm (STP, 273 K and 1 atm, cm^3 min^{-1}) N_2, over a drop of liquid CH_3SO_3H placed in a bend near the end of the injector (depicted in Figure 1a). Reactant H_2SO_4 was formed in situ by reaction of OH with SO_2 (the product HSO_3 rapidly forms H_2SO_4 in the presence of

10.1021/jp0510443 CCC: $30.25
Published on Web 07/15/2005

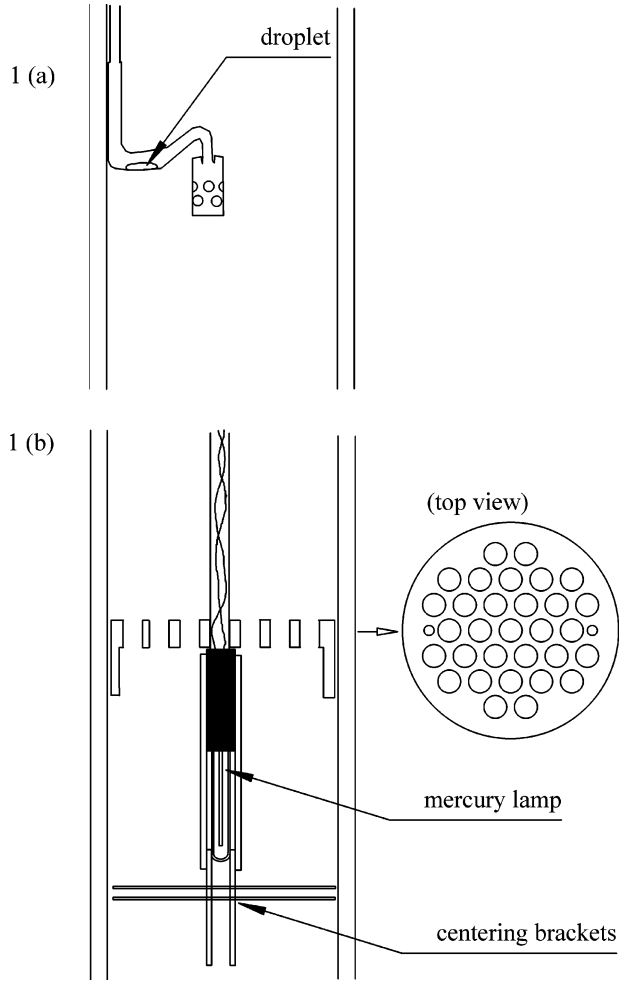

Figure 1. Schematic drawings of the reactant sources: (a) CH_3SO_3H liquid droplet in a showerhead-type injector, and (b) the OH + SO_2 source for H_2SO_4, where an encapsulated Hg PenRay lamp emits 185 nm light that dissociates H_2O to produce OH. A Teflon flow straightener was located just above the lamp. For most of the measurements, a coil of stainless steel shim (not shown) was placed over the Teflon encapsulating the lamp to decrease the UV light to limit the production of H_2SO_4.

O_2 and H_2O[52]). OH was formed by irradiation of H_2O with 185 nm light from a small mercury lamp (2.5 cm long × 0.5 cm in diameter, encapsulated in a 3/8" o.d. Teflon tube) suspended along the center axis of the flow reactor (shown in Figure 1b). SO_2 was taken from dilute (0.1−0.5%) SO_2-in-N_2 mixtures and [SO_2] in the flow reactor were estimated from the relative flows to be 3×10^{10} to 10^{12} cm^{-3}. A perforated Teflon disk directly above the mercury lamp (Figure 1b) suppressed eddies that could be induced in the flow reactor due to the ∼1 W of heat from the lamp. The lamp was operated at low power to limit the heating of the gas within the flow reactor and the amount of H_2SO_4 formed. At high [H_2SO_4], the formation of small particles was observed, presumably due to nucleation involving H_2SO_4, and they were primarily confined to the central axis (r < 0.7 cm) of the flow reactor. For many of the measurements, especially those at high RH, an additional decrease in UV light (thus less nucleation) was accomplished by surrounding the lamp with a stainless steel spiral. For most of the measurements, these particles were present at less than 100 cm^{-3}, while a few uptake measurements were conducted with up to 1000 cm^{-3} (central axis value) present. Note that these are very small particles, ∼5 nm in diameter, with an insignificant surface area and thus they did not significantly affect the measured H_2SO_4 first-order loss rate coefficients.

The thermostated flow reactor was held at 295 (±0.3) K for the H_2SO_4 experiments and 295−297.5 K for the MSA experiments and was operated at pressures of 605−623 Torr total pressure. Total flow rate of N_2 was 1800 to 2100 sccm (except for two H_2SO_4 wall loss determinations at RH = 0.275 the mass flow rate was 4000 sccm), the average linear flow velocity V_{ave} was 2−2.4 cm s^{-1}, and the Reynold's number was ∼60. An additional flow of 50−100 sccm of O_2 (UHP) was used in the H_2SO_4 measurements.

The particles were formed by rapid cooling (from ∼110 C to room temperature) of a flow of H_2SO_4 vapor-in-N_2 (100 sccm). Up to 10 sccm of this flow was mixed with the humidified main flow to yield the aerosol. The distribution of particle sizes was well characterized by a log-normal distribution with peak radii ranging from 50−120 nm and lnσ was typically 0.28. The DMA sheath flow was ∼1800 sccm and was humidified to ∼11% RH, and sample and monodisperse flows were ∼230 sccm. Note that an additional uncertainty is assigned to the data because the aerosol dries out during its transit of the DMA. See note *d* in Table 1 for more discussion. The overall number density of particles, N_p, ranged from 0.4 to 7 × 10^4 cm^{-3}. The particle counter sampled aerosol at a flow rate of 1−1.5 cm^3/s, and this was diluted with ∼22 cm^3/s N_2 diluent gas added in a sheath arrangement. For the H_2SO_4 measurements, gas-phase SO_2 in the particle charger (1.2 mCi of ^{241}Am in a volume of ∼100 cm^3) interacted with OH and/or ions[20−22] and led to the formation of small (5−20 nm diameter) particles. These were easily separated from the ∼150 nm diameter aerosol particles that were responsible for the uptake. See the appendix for a detailed discussion of the formation of these small particles.

The measured particle size distribution was not affected by the presence of H_2SO_4. Thus the size of the particles was not significantly altered by the uptake of the acids. This is consistent with the estimate presented below of the maximum [H_2SO_4] (radially averaged) of 3×10^9 cm^{-3}, whereas the particles contained the equivalent of 2−6 × 10^{11} acid molecules cm^{-3}. For the MSA experiments, a larger acid concentration was present for the uptake measurements, estimated to be as high as ∼3×10^{10} cm^{-3}. Thus a significant swelling of the particles (∼10% in volume) could have taken place due to MSA uptake (unlike the H_2SO_4 experiments, a specific test designed to detect a swelling effect upon addition of MSA was not performed). Because the particle size distribution was monitored during the uptake measurements, this potential swelling would be taken into account in the determination of α.

The chemical ionization region was altered slightly from that depicted in Fig. 1 of ref. 19 and it is very similar to that depicted in Figure 2b of reference 24: the drift region is 8.5 cm long and has five annular ion guide lenses spaced at 1.7 cm intervals.

Reactant H_2SO_4 and CH_3SO_3H were monitored by converting them to HSO_4^- and $CH_3SO_3^-$ ions, respectively, via reaction with NO_3^-·HNO_3 ions. N_2 (40−100 sccm) containing a trace of HNO_3 vapor (∼0.1−1 ppmv) was flowed through the source to yield NO_3^-·HNO_3 ions. Both reactants are stronger gas-phase acids than nitric acid; thus, the reactions

$$H_2SO_4 + NO_3^-\cdot HNO_3 \rightarrow HSO_4^-\cdot HNO_3 + HNO_3 \quad (1)$$

$$CH_3SO_3H + NO_3^-\cdot HNO_3 \rightarrow CH_3SO_3^-\cdot HNO_3 + HNO_3 \quad (2)$$

are facile with rate coefficients of ∼$2-3 \times 10^{-9}$ cm^3 s^{-1}.[25,26] The ion products were present primarily with an attached HNO_3

TABLE 1: H_2SO_4 Experimental Parameters and Uptake Results[a]

RH	wt %,[b] H_2SO_4	k_z, cm^{-1}	N_p, 10^4 cm^{-3}	r_s,[c] 10^{-6} cm	X_{SA},[d] factor	k_m,[e] s^{-1}	γ_{ex}[f]	γ[g]	$+\Delta\gamma$[h]	$-\Delta\gamma$[h]
0.056	68.5	0.0377	2.20	7.01	0.93	0.045	0.65	0.80	0.19	0.15
0.060	68.0	0.0529	5.35	6.80	0.94	0.099	0.63	0.75	0.13	0.10
0.060	68.0	0.0484	5.13	6.59	0.94	0.083	0.55	0.64	0.11	0.09
0.060	68.0	0.0349	2.11	6.79	0.94	0.035	0.57	0.67	0.18	0.14
0.114	63.1	0.0426	3.46	6.28	1.00	0.058	0.66	0.77	0.16	0.13
0.265	54.0	0.0388	2.47	7.66	1.14	0.055	0.59	0.74	0.18	0.14
0.272	53.7	0.0407	2.50	7.91	1.15	0.062	0.63	0.81	0.20	0.15
0.462	44.7	0.0392	2.87	7.33	1.34	0.054	0.56	0.67	0.18	0.14
0.462	44.7	0.0570	4.92	7.40	1.34	0.117	0.69	0.88	0.20	0.16
0.495	43.0	0.0366	2.03	7.63	1.36	0.045	0.60	0.74	0.23	0.17
0.495	43.0	0.0334	1.33	7.67	1.36	0.034	0.70	0.90	0.33	0.23
0.632	36.6	0.0433	2.04	7.87	1.56	0.073	0.91	1.34	0.44	0.31
0.636	36.4	0.0554	4.52	7.89	1.57	0.116	0.65	0.84	0.22	0.17
0.638	36.3	0.0418	4.08	6.04	1.54	0.077	0.82	1.04	0.29	0.22
0.638	36.3	0.0549	7.92	6.12	1.54	0.127	0.68	0.83	0.20	0.16
0.707	32.6	0.0388	1.59	8.48	1.70	0.059	0.82	1.22	0.45	0.31
0.744	30.4	0.0588	3.64	8.21	1.80	0.129	0.83	1.21	0.38	0.28
0.804	26.4	0.0451	5.19	6.67	1.97	0.087	0.60	0.72	0.21	0.16
0.804	26.4	0.0452	5.37	6.67	1.97	0.088	0.59	0.70	0.20	0.15
0.846	23.1	0.0499	2.85	9.33	2.22	0.101	0.65	0.91	0.32	0.22
0.863	21.6	0.0669	4.76	9.36	2.34	0.161	0.61	0.83	0.28	0.20

[a] Temperature was 295 ± 0.3 K, total pressure (>95% N_2) was 615 ± 10 Torr, and V_{ave}, the average carrier velocity, was 2.2 ± 0.2 cm/s. [b] H_2SO_4 content of the particles in the flow reactor calculated using the data on the AIM[28] website.[54] [c] Surface-area-weighted radius of the particles in the flow reactor: $r_s = r_p \exp(2.5*[\ln \sigma]^2)$, where r_p is the peak radius of the log-normal distribution and $\ln \sigma$ is the standard deviation (ref 19 and references therein). [d] The particle sizes in the flow reactor are different than in the differential mobility analyzer (DMA) where the sheath flow was maintained at 10% RH. The H_2SO_4 content of the particles in the DMA varied slightly due to RH variation of aerosol sample flow (between 55 and 65 wt %). This factor[19] X_{SA} is calculated from the known water contents and measured temperatures and assuming the aerosol experienced an instantaneous change in RH (and thus particle size) upon entering the DMA. The density of sulfuric acid solutions, needed to calculate this factor, were given by $\rho = -4.157 \times 10^{-7} wp^3 + 9.015 \times 10^{-5} wp^2 + 4.15410^{-3} wp + 1.0195$, the result of a polynomial fit to the data in ref 49 for 10−90 wt % H_2SO_4 solutions at 295 K. It is within 0.5% of the density given by Huthwelker et al.[50] As discussed in the text and in ref 19, an additional uncertainty to γ arises that is based on an uncertainty in surface area due to a 1.5% variation in flow reactor RH: $\Delta SA/SA(\%) = 0.25(X_{SA})^3$. An uncertainty due to changes in particle size within the DMA (see the text) was found to follow: $\Delta SA/SA(\%) = 12*RH$. These two were simply added to obtain the uncertainty in γ.[54] [e] The first-order loss rate coefficient due to uptake onto the particles. It was calculated from $k_m = 1.61*(V_{ave}*k_z - k_w)$. [f] From eqs 3 and 4. [g] The diffusion-corrected uptake coefficient (from eq 5) and $\lambda(r_s) = (0.75+0.283Kn_{rs})/(Kn_{rs}(Kn_{rs}+1))$, where $Kn_{rs} = 3D_c/\omega r_s$ (refs 19 and 33). [h] Positive and negative error bars in γ. Two sources were combined quadratically, (i) $\Delta k_m/k_m$ that ranged from 7% to 20% and (ii) ∼8% precision in determining aerosol surface area. Additionally, the two sources of $\Delta SA/SA$ from note *d* were added to this quantity. For this latter quantity, the particle size was varied and it compensated somewhat for the variation of γ with ΔSA via changes in the quantity $\lambda(r_s)$.

ligand as denoted in eqs 1 and 2, although depending upon relative humidity, significant (>10%) signals were observed at the core ion masses and those that corresponded to attached H_2O ligands. Ion−molecule reaction time was 5−10 ms, and for the reactant concentrations present at the level of the ion drift region, the reagent ion signal was depleted by < 10% (<8% for CH_3SO_3H and <1% for H_2SO_4). The measured [reactant] (a radially averaged value) was as high as 1×10^9 cm^{-3} for the H_2SO_4 measurements and as high as 6×10^9 cm^{-3} for the MSA experiments, estimated from the ion−molecule reaction time and rate coefficient. Because of losses on surfaces between the acid source and the detection region such as the flow reactor wall and ion guides, the reactant concentration near the source in the center of the reactor was likely to be much (3−10 times) higher than this.

Decays were determined from the CIMS signals recorded at reactant-particle interaction lengths of 25−90 cm. Note that the shortest length is significantly longer than the 15 cm entrance length and the vast majority of data was outside the ∼25−30 cm mixing length.[27] Frequently, the particles were turned off, and wall loss measurements were taken at flow rates and RH similar to those in existence when particles were present. Determining the wall loss rate coefficient leads to an accurate determination of the mass accommodation coefficient because the loss on the wall must be subtracted from the measured loss when particles are present. Measurements of the wall loss rate coefficient also allow for the determination of the diffusion coefficient. A good agreement of the diffusion coefficient determined in this way with previously reported values can also provide further validation that fully developed laminar flow was not compromised by the heat from the lamp.

There was a small background signal for HSO_4^- ions with the mercury lamp off that depended upon $[SO_2]$ and was suppressed upon addition of propane to the source flow. Thus, it was likely due to processes within the ion source, possibly from OH generated by α-particles reacting with SO_2 near to the exit of the ion-source. It ranged between 2% and 20% of the signal due to the H_2SO_4 in the flow reactor. In the data analysis, the background ion signal was subtracted from the signal measured during the kinetics runs to obtain the first-order loss rate coefficient or it was included as a parameter in a weighted least-squares fitting routine. For the CH_3SO_3H measurements, the background signal was on the order of 1% or less of the signal due to initial $[CH_3SO_3H]$.

An additional background signal is expected from acid vapor eluting from surfaces such as the flow reactor wall and ion lenses. We did not observe a signal that could be unequivocally attributed to reactor surfaces even though the bulk H_2SO_4 vapor pressure (2×10^{-12} atm)[28] for the low relative humidity experiments (RH = 6%) indicates it should have been detectable. Conclusions regarding the allotment of the background signal to "contaminated" surfaces or OH production in the ion source are difficult because of their dependencies upon relative humidity. However, there was also no significant background signal observed for MSA at low RH which indicates that the acid coverage of the reactor surfaces (estimated to be $\ll 10^{14}$

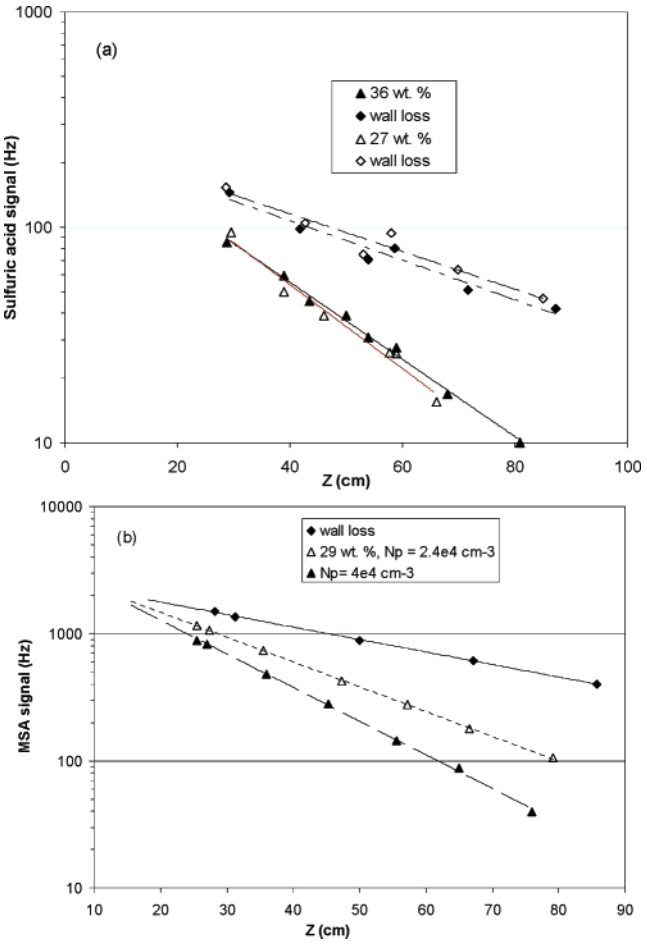

Figure 2. Signals due to (a) H_2SO_4 and (b) CH_3SO_3H as they were exposed to the wall (in the absence of particles, diamonds) and additionally to particles (triangles). The axial decay constant is obtained from the slope of the least-squares fits to the data. For panel a, the filled and open symbols are the signals in the presence of 36 and 27 wt % H_2SO_4 particles, respectively. For panel b, the filled and open triangles are the signals in the presence of two different number densities of 29 wt % H_2SO_4 particles.

cm^{-2}) was not sufficient to express their bulk partial pressures. Yet the H_2SO_4 partial pressures exhibited by the particles were detectable (see below).

The solubilities of H_2SO_4 and CH_3SO_3H in dilute sulfuric acid are large enough[8,28] such that desorption was in general insignificant for experiments at >10% RH for H_2SO_4 and >40% RH for CH_3SO_3H. For H_2SO_4, desorption effects can be estimated from the saturated vapor pressure of H_2SO_4 over its aqueous solutions.[28] The H_2SO_4 partial pressure increases with the H_2SO_4–content of the solution, with the largest value for ~68 wt % H_2SO_4 that corresponds to $\sim 4 \times 10^7$ cm^{-3}. A background signal at about 20−40% of this level was observed that depended upon the particle number density. A loss process that depletes the vapor pressure over the particles, such as a first-order loss on the ion guides, could provide an explanation for this dependence, the mechanism being that the ion guides are an efficient scavenger of gas-phase H_2SO_4, and the resupply of gas-phase H_2SO_4 to the ion drift region is limited by the available particle surface area. However, uncertainties in calculated H_2SO_4 vapor pressures are large and preclude a definite conclusion.

For CH_3SO_3H, with a Henry's law coefficient in water of $\sim 10^{14}$ $molal^2/atm$ at 295 K,[8] the solubility is very high in dilute H_2SO_4 solutions. Up to H_2SO_4–contents of 40 wt % where $[H^+]$ is ~5 molal and the activity coefficients are likely 10 or less,[28,29] desorption effects can probably be neglected. However, desorption effects were evident for measurements where solutions contained 50 wt % or greater H_2SO_4 (33% RH or less), indicating that the effective Henry's law coefficient is decreased due to increasing acid concentration and significant (factors of 10 or larger) departures of the activity coefficients from unity.[29]

Any species taken up can diffuse throughout these small particles very rapidly, on the order of 10^{-4} s.[19] Water vapor, present in large excess, is expected to accompany the incorporation of the acids into solution. Furthermore, the surface of dilute acids, even though the acid molecule is present at the surface in excess over its bulk concentration, is believed to be primarily composed of water molecules.[30,31] Thus CH_3SO_3H and H_2SO_4, once taken up, likely travel into the bulk of the solution. Because the uptake is due to incorporation into the bulk of the particle, it can be identified with the mass accommodation process. Furthermore, if it is known that desorption is not occurring at a significant rate, then the value of the measured uptake coefficient γ is also the value for α.

Results and Analysis

Typical kinetic data are shown in Figure 2a, a semilog plot of the signal at 160 amu (HSO_4^-·) vs injector position for loss of H_2SO_4 onto the reactor wall only (diamonds) and for the additional loss onto particles composed of 27 and 36 wt % H_2SO_4 (triangles, respectively). Figure 2b shows similar data for CH_3SO_3H uptake (sum of the signals at 95, 158, and 221 amu vs injector position) onto the wall and additionally onto particles. The measured background signals have been subtracted from the data. It is apparent from these plots that the losses are characteristic of first-order processes.

The value of the mass accommodation coefficient α was extracted from the measured decay coefficients and particle size distributions as detailed in ref 19. To summarize, the measured first-order loss rate coefficient that is due to uptake onto particles, k_m, is calculated from the difference between decays with and without particles present. For example, assuming V_{ave} does not vary significantly when the particle flow was turned on, k_m is equal to V_{ave} × the difference in slopes in Figure 2 for data with particles present and for particles absent. This is multiplied by a factor of ~1.6 to account for radial concentration gradients and laminar flow (the axial concentration gradient correction factor[19] was neglected, as it is less than 2%). Division of k_m by the first-order collision rate of the acid with particles k_c yields a value for the extracted reaction probability, γ_{ex}. The diffusion resistance and the deviation of the distribution of molecular speeds from a Maxwellian distribution are then taken into account according to the Fuchs-Sutugin[33] equation (represented by $\lambda(r)$, see Table 1), where the value of the Knudsen number is taken at the surface area-weighted radius, r_s,[19,34] (see note *c* in Table 1). In this way a value for the uptake coefficient γ, which can be equivalent to α, is obtained

$$k_c = \frac{\omega}{4} SA_f = \omega N_p \pi r_p^2 \exp(2 \ln \sigma^2) \quad (3)$$

$$\gamma_{ex} = \frac{k_m}{k_c} \quad (4)$$

$$\frac{1}{\gamma} = \frac{1}{\gamma_{ex}} - \lambda(r_s) \quad (5)$$

where ω is the mean molecular speed of the reactant and SA_f is the aerosol surface area density in the flow reactor. For the

TABLE 2: CH_3SO_3H Uptake Experimental Conditions and Results[a]

RH	wt %,[b] H_2SO_4	k_z, cm^{-1}	N_p, 10^4 cm^{-3}	r_s,[c] 10^{-6} cm	SA,[d] factor	k_m,[e] s^{-1}	γ_{ex}[f]	γ[g]	$+\Delta\gamma$[h]	$-\Delta\gamma$[h]
0.092	65.0	0.035[e]	10.0	5.00	1.00	0.037	0.23[i]	0.25[i]	0.05	0.04
0.230	56.0	0.0259	2.37	7.17	1.05	0.0043	0.04[j]	0.04[j]	0.06	0.02
0.338	50.2	0.0289	0.55	10.2	1.26	0.0181	0.52	0.69	0.36	0.22
0.338	50.2	0.0409	1.90	10.2	1.26	0.0598	0.49	0.64	0.16	0.12
0.338	50.2	0.0323	0.98	10.2	1.26	0.0299	0.48	0.63	0.22	0.16
0.414	47.0	0.0366	0.51	10.8	1.33	0.0313	0.65	0.93[k]	0.32	0.22
0.586	38.8	0.0562	7.26	6.05	1.48	0.171	0.65	0.76	0.18	0.14
0.586	38.8	0.0478	4.50	6.05	1.48	0.106	0.77	0.93	0.24	0.19
0.698	33.0	0.0418	0.96	12.2	1.79	0.0605	0.70	1.18	0.48	0.31
0.749	30.1	0.0338	1.03	10.2	1.77	0.0380	0.58	0.79	0.33	0.22
0.759	29.5	0.0453	2.37	9.74	1.80	0.0790	0.57	0.76	0.24	0.18
0.773	28.6	0.0612	3.97	9.53	1.84	0.136	0.62	0.85	0.26	0.19
0.874	20.4	0.0291	0.37	12.7	2.42	0.0220	0.60	0.96	0.73	0.37
0.879	20.0	0.0531	2.70	11.0	2.46	0.107	0.53	0.74	0.27	0.19
0.884	19.6	0.0379	1.07	12.0	2.50	0.0532	0.56	0.84	0.39	0.25
0.891	18.8	0.0553	4.66	8.05	2.61	0.194	0.58	0.72	0.24	0.18
0.926	14.7	0.0476	1.72	12.0	3.05	0.0875	0.57	0.99	0.54	0.32
0.934	13.5	0.0373	0.87	13.3	3.24	0.0508	0.53	0.96	0.67	0.35
0.937	13.1	0.0629	2.74	11.5	3.32	0.142	0.56	0.94	0.49	0.30
0.970	7.2	0.079	4.62	11.6	5.51	0.4058	0.51	0.69	0.60	0.30

[a] Temperature was 296.2 ± 1.3 K, total pressure (>95% N_2) was 618 ± 8 Torr, and average carrier velocity was 2.2 ± 0.2 cm/s. [b–h] See Table 1 notes. [i] Loss estimated from initial data point; later data showed evidence of desorption such that γ_{ex} would be negative. [j] Upper limit; CH_3SO_3H signal was not significantly perturbed by interaction with particles. [k] Uptake data obtained with DMA situated upstream of flow reactor thus distribution of particles was very narrow and sizable fraction of particles were likely to have remained charged during the measurement. Measured N_p varied (±20%) reproducibly with injector position presumably due to loss of charged particles on Teflon injector line.

present measurements, the Fuchs−Sutugin correction (eq 5 and note *g* in Table 1) amounted to 5−50% of the resulting γ (or α.)

Shown in Tables 1 and 2 are lists of experimental parameters and the measured kinetic values and the resulting values of α for H_2SO_4 and γ for CH_3SO_3H, respectively. Notes in the Tables give detailed information on these parameters and their analysis. The resulting uptake coefficients are plotted versus relative humidity in Figure 3a,b. It is clear that over a majority of the RH range, the uptake of these species indicates an efficient incorporation into the bulk of the particles.

For the H_2SO_4 measurements, the average value for α is 0.86 ± 0.08 (21 points) and there could be a trend with RH: for RH < 0.5, the average α is 0.76 ± 0.05 (11 points), and that for RH > 0.6 is 0.96 ± 0.14. These averages are nonweighted, and the quoted errors are twice the standard errors of the mean (the standard deviation of the sample divided by the square root of the number of points). See below for a discussion of the overall measurement uncertainties.

For CH_3SO_3H, the average value for the uptake coefficient is 0.86 (±0.08, twice the standard error of the mean) for the data between 40% and 90% RH (11 points). The average of four results at RH > 92% is $\gamma = 0.89$, which is not significantly different than that for the lower RH data; however, these data have large uncertainties (see below). The scatter in the individual data points is somewhat less than that for H_2SO_4 in part because a relatively higher [CH_3SO_3H] could be used. It is likely that the uptake was not influenced by desorption for these conditions[29]; thus, γ can be identified with the mass accommodation coefficient α. For RH < 0.4, the data show that a low value for γ can describe the kinetics, which probably indicates significant desorption was occurring due to a low value for the solubility[29] of CH_3SO_3H in the more acidic particles.

Each individual determination of the mass accommodation coefficient was measured to a typical precision of ±11−28% (for CH_3SO_3H and RH > 0.4) and ±14−27% (H_2SO_4). These are due to the precision of the k_m (7−27% due to the 3.5% error in k_w and 5−7% error in k_z) and of the surface area determination (8%). See ref 19 for a detailed breakdown of the typical sources of scatter. There is an accuracy uncertainty of ±10% in determining the absolute N_p using a TSI 3760.[19] This uncertainty was not included in the errors listed in the Tables or shown in Figure 3a,b.

There is additional uncertainty in the surface area due to the fact that the RH in the flow reactor can be quite different than that in the DMA. There are two different sources of uncertainty: (1) Because of the estimated uncertainty in flow reactor RH of 1.5% (i.e., using a multiplying factor for RH of 1.015 and 0.985, equivalent to a ±0.3 K temperature uncertainty), the uncertainty in the quantity X_{SA} and thus surface area is 1%, 2.5%, 7%, 20%, and 40% at RH = 0.6, 0.8, 0.9, 0.95, and 0.97, respectively. These were estimated from the equations in the notes to Table 1 and ref 28. (2) Because of the drying of the aerosol within the DMA and consequent changes in the sizes of the particles, a small uncertainty arises in the calculated size distribution. This is because the calculation is based on a particle's size remaining constant during its transit of the DMA. It is difficult to predict a particle's RH history because it will be drawn out of the high RH region into a lower RH region while at the same time water vapor is diffusing throughout the DMA. The contribution of this effect to the uncertainty in surface area was estimated by calculating the relative size change in the particles had they been introduced at the same RH as the sheath flow. To a good approximation, the uncertainty in surface area scales linearly with RH and it is about 10% at RH = 90%.[54]

For the H_2SO_4 data, the surface area error due to the RH uncertainty is less than 7% for the data at RH ≤ 0.5, and it ranges from 8−14% for the data at RH ≥ 0.63. Adding in (14% and 21%) accuracy uncertainties to the values of γ_{ex} results in asymmetric uncertainties in the resulting values for γ due to eq 5. The resulting errors in the average values for the mass accommodation coefficients are 0.76 (+0.17/−0.16) and 0.96 (+0.37/−0.35) for the RH < 0.5 and RH > 0.6 data, respectively.

The CH_3SO_3H data from 40 to 90% RH had additional surface area uncertainty that ranged from 5−15%. A few of the CH_3SO_3H measurements (those with RH ≥ 0.93) had additional error in the surface area that exceeded 15%. This is

the reason that the average value reported above was limited to RH < 0.9. The full uncertainty in α for CH_3SO_3H can be obtained by adding in a ∼20% systematic uncertainty (∼10% surface area, 10% in N_p) to obtain α = 0.86 (+0.31/−0.26) for 0.4 < RH < 0.9.

A value for the gas-phase diffusion coefficient can be obtained in the absence of particles because diffusion controls the loss of the gas-phase species onto the reactor walls. Shown in Figure 4a, b are the diffusion coefficients for the acids extracted from the first-order wall loss rate coefficients (the procedure is detailed in ref 32). As discussed in ref 32, the substitution of up to 3% H_2O vapor for N_2 would give a result that is negligibly different than if 100% N_2 were present (aside from, of course, affecting the extent of hydration). We assume similar arguments can be made regarding the 2−5% O_2 that was present for the H_2SO_4 measurements. Thus the total pressure was used to convert the measured diffusion coefficient D_c to the pressure independent diffusion coefficient pD_c for the reactant diffusing through N_2.

Discussion

Mass Accommodation. Recently published measurements of α for H_2SO_4 are shown as filled symbols in Figure 3a. While good agreement is exhibited for the more concentrated solutions at low RH (<0.1),[15,16] the previous data at 50% RH[14] is not in good agreement with the present results. These previous results were obtained from calculated concentrations (i.e., [H_2SO_4] was not monitored directly), and perhaps some unknown or neglected chemistry had a large effect on the calculated [H_2SO_4].

For CH_3SO_3H, the present data indicates that it is efficiently taken up when its solubility (i.e., Henry's law coefficient) is high. Because CH_3SO_3H solubility should be very high in neat aqueous solutions, there is an apparent disagreement with the previously[17,18] reported values for α of 0.1 at 100% RH.

The present results for the mass accommodation coefficients for H_2SO_4 and CH_3SO_3H suggest that particle growth rates due to these species are not limited by α. Likewise, calculated loss rates for H_2SO_4 or CH_3SO_3H due to uptake onto aerosol particles are not limited by α. This was also the conclusion of two of the previous laboratory studies[15,16] for uptake at low RH. The uptake efficiency of H_2SO_4 of $\gamma \sim 0.5$ inferred from two field studies[6,7] at high RH are more in agreement with the present results than the value for α of 0.045 from the previous laboratory work at 50% RH.

These results are consistent with a picture of mass accommodation where a very low fraction of molecules are excluded from entering the bulk of aqueous solutions, a picture that has been previously substantiated for HCl[35] and NH_3[19] from experiments in aerosol flow reactors. This picture is not in accord with that derived from results using the droplet train apparatus (e.g., refs 36 and 37). There is an ongoing debate regarding the accuracy of these conflicting experiments.[19,38−46] It suffices to say that this debate has not yet been satisfactorily resolved.

Diffusion Coefficients. The diffusion coefficient for H_2SO_4 has a marked dependence upon relative humidity. The curve in Figure 4a is taken from ref 32 but with a value for pD_c = 0.088 atm cm^2/s for neat H_2SO_4 in N_2 at 295 K. It is assumed that the thermodynamic equilibrium constants for hydration vary with temperature assuming that each H_2O is bound by 10 kcal/mol. This is close to the latent heat of evaporation of water; thus, this assumption is equivalent to assuming negligible change with temperature in the variation of diffusion rates with RH. Please see ref 32 for further details. This value for pD_c for neat H_2SO_4 is about 6% less than that reported at 298 K[32], and the temperature difference can account for about 1/3 of the difference. Thus, the two sets of measurements are different on average by about 4%, well within the measurement uncertainties. Agreement within the quoted uncertainties is also seen with other previously determined values at 303 K[16] of 0.088 (±2%) atm cm^2/s and 295 K[53] of 0.11 (±20%) atm cm^2/s.

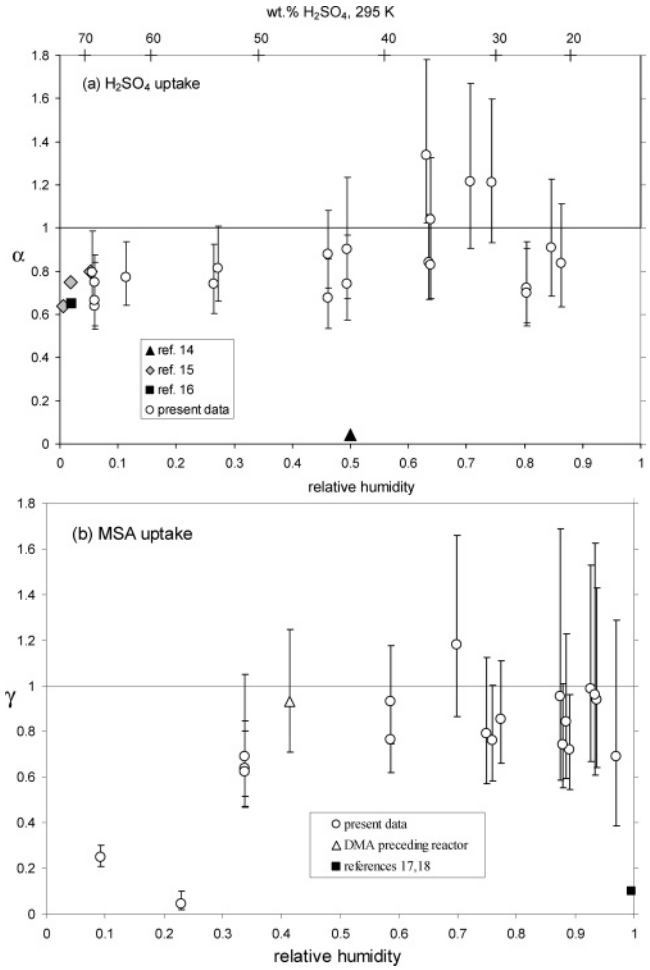

Figure 3. The resulting diffusion-corrected uptake coefficients for (a) H_2SO_4 and (b) CH_3SO_3H plotted vs RH. This quantity is identified as the mass accommodation coefficient for the H_2SO_4 results and for the CH_3SO_3H results above RH = 0.4. There are significant desorption effects for the CH_3SO_3H results at low RH. Previously reported measurements at low RH (<0.12) for H_2SO_4 are shown as the filled square and triangles[15,16] and at RH = 0.5 as the filled diamond.[14] The filled square is the α for CH_3SO_3H reported at RH = 1 of ∼0.10 for 296 K.[17,18]

The variation of pD_c with RH here is well-described by the function derived from previous measurements.[32] With calculated changes of ∼15% and ∼ 27% in the diffusivity of H_2SO_4 when it has one and two waters of hydration, respectively, this variation was explained as follows: half the H_2SO_4 molecules possess ∼1 water of hydration near 10% RH, and then accumulation of a second one leads to equal number densities of the mono and dihydrates at around 50% RH.[32] Recent work[47] on the hydration of H_2SO_4 obtained by comparing theory to other experimental results is consistent with the present and previous[32] measurements. Wall loss measurements were taken over a wider range of conditions than for the uptake measurements and the data point at ∼92% RH appears to be an outlier. Further measurements under these conditions are needed to evaluate the detection of additional waters of hydration of H_2SO_4.

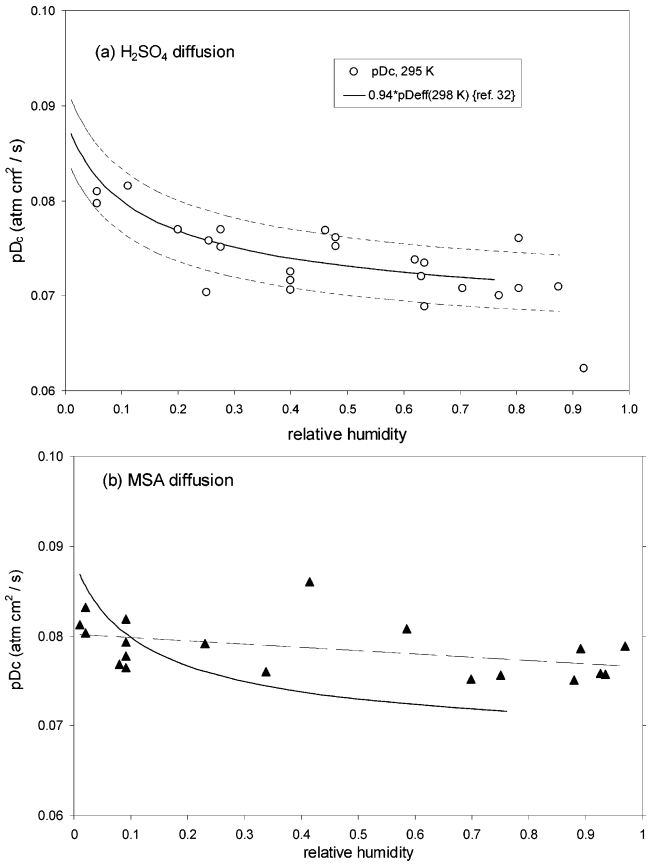

Figure 4. Pressure independent diffusion coefficients, pD_c, for H_2SO_4 (a) and CH_3SO_3H (b) plotted vs RH. The D_c were obtained from the measured wall loss rate coefficients k_w, by equating it to the theoretical diffusion-limited loss rate coefficients for laminar flow in a cylindrical flow reactor given by $3.65D_c/a^2$, where D_c is the diffusion coefficient and a is the reactor diameter (see refs 19 and 32 and references therein).

As can be seen in Figure 4b, pD_c for CH_3SO_3H does not have a significant dependence on RH. A linear fit, shown as the dashed line, indicates a ~3% decrease in the diffusion coefficient over this range of RH. The curve from Figure 4a is reproduced to illustrate the difference between the measurements: this curve decreases ~ 17% from RH = 0.02 to 0.8. We obtain an average value of 0.0786 atm cm^2 s^{-1}, or 0.080 if the intercept of the dashed line is used, for the pressure independent diffusion coefficient for CH_3SO_3H in N_2 at 296.2 ± 1.2 K. A slightly larger size for CH_3SO_3H versus H_2SO_4[48] could be responsible for the ~ 10% difference in pD_c.

Conclusions

The present measurements show that the mass accommodation coefficients of H_2SO_4 and CH_3SO_3H onto dilute sulfuric acid droplets are essentially unity. The average values measured for α for these species is consistent with unit uptake efficiency. Therefore, in calculations of aerosol growth via uptake of H_2SO_4 and CH_3SO_3H (as well as NH_3[19]), an α near unity is supported by results from aerosol flow reactors. Note that uptake of H_2SO_4 by aerosol particles that is more efficient than previously thought can diminish the connection between DMS and the number density of cloud-condensation nuclei.[1−5] This could be due to a suppression of atmospheric [H_2SO_4] via uptake onto preexisting aerosol[51] and the consequent suppression of nucleating particles that become cloud nuclei.

The values of the H_2SO_4 diffusion coefficient and its variation with RH compare favorably with previous measurements. The present measurements support the explanation of the variation of pD_c with RH as due to the hydration of an H_2SO_4 molecule with one and then two water molecules as RH increases. The CH_3SO_3H diffusion coefficients are much less dependent upon RH which indicates that hydration of CH_3SO_3H is not significant over this range.

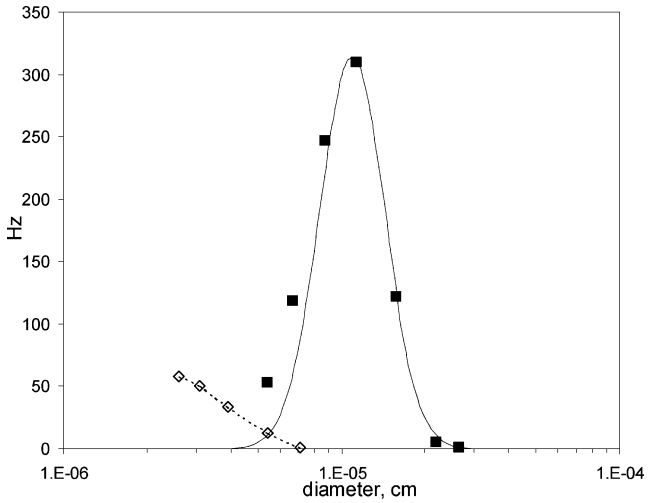

Figure 5. Output of a particle counter at the monodisperse outlet of the DMA for large particles present (squares) and large particles absent (diamonds).

It has been argued previously[19,38−44] that the droplet train results can be interpreted in such a manner as to be consistent with a highly efficient mass accommodation process, although these assertions have not gained acceptance.[45,46] The controversy continues in part because of the inherent difficulties of separating out the effects of the multitude of mass transfer processes that can be present in any real experimental apparatus.

Acknowledgment. We thank J. Smith for use of the 3020 CNC and 3025A ultrafine CNC. Comments on the text by J. Orlando, J. Smith and the anonymous reviewers were very helpful in improving the manuscript.

Appendix

We observed particle formation when SO_2 was present inside particle chargers that employed ^{241}Am and ^{210}Po radioactive ion sources. Detailed here are results from particles formed in a charger that had a volume of ~100 cm^3. Primarily a 1.2 mCi ^{241}Am ion source was used. The charger was used in two ways: (i) on the inlet to the DMA to charge the particles for sizing as in the uptake experiments and (ii) on the inlet of a particle counter.

Shown in Figure 5 are size distributions measured for two conditions: aerosol particles with ~14 ppbv SO_2 present; ~14 ppbv SO_2 present only. Relative humidity in the charger was ~70% and gas residence time was ~20 s. It is clear that these two are well separated in diameter and thus the aerosol size distribution in the flow reactor can be readily extracted. Furthermore, most of the experiments on H_2SO_4 uptake were performed with [SO_2] at levels much lower than 14 ppbv and distributions measured under these conditions showed much lower particle concentrations at diameters of 6×10^{-6} cm and less.

In another series of experiments, particle production within the charger at various SO_2 and RH levels was investigated. Also, either CH_4 or C_3H_8 was introduced with the sample flow, whereupon particle production was reduced markedly. The

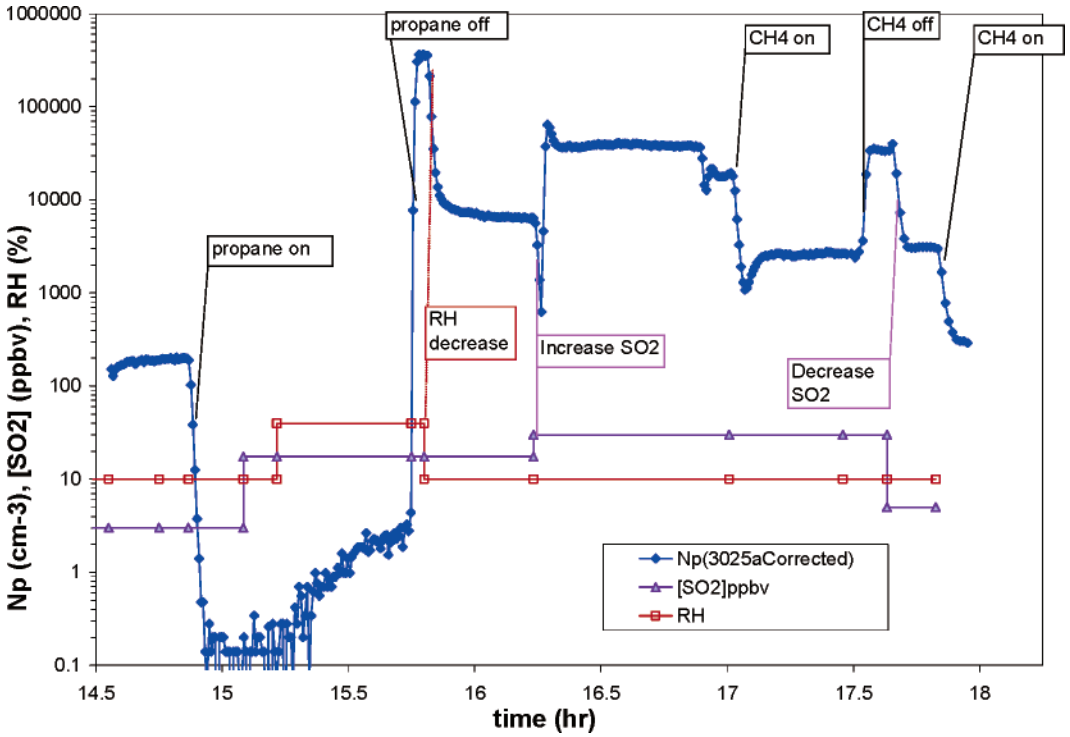

Figure 6. Number density of small particles (diamonds), calculated SO_2 levels (triangle), and relative humidity (squares) plotted as a function of time. The changes in other experimental conditions that are indicated in the figure are detailed in the appendix.

results of these experiments are depicted in Figure 6, a plot of the output of a TSI-3025A (an ultrafine condensation nuclei counter, cm^{-3}), RH (%), and [SO_2] (ppbv) versus time. Note that the residence time in the charger for these experiments was ~4 s, much shorter than for the uptake experiments, as the 3025A drew a larger flow (~25 vs 5 cm^3/s for a TSI 3020).

In Figure 6, initially the 3025a reported a particle number density, N_p, of ~200 cm^{-3} for an RH of 10% and an [SO_2] of 3 ppbv. Upon the addition of several tens of ppmv propane (~15 h), these particles were greatly reduced, presumably through scavenging of OH radicals. While propane was present, SO_2 and RH were increased to 18 ppbv and 40%, respectively; yet N_p increased only modestly during this time (propane had unintentionally decreased during this time, to ~ 10 ppmv). That a large suppression of particle generation by propane was still taking place is seen by a ~10^5 fold increase in N_p upon taking propane away. Later on, at ~17 h and again at ~17.8 h, the addition of ~12 ppmv methane is shown, and N_p was observed to decrease 10-fold. In another set of experiments using a ^{210}Po charger (0.6 mCi, ~ 100 cm^3 volume), a 50-fold reduction in N_p was observed upon addition of 250 ppmv CH_4, while addition of 2 ppmv propane resulted in a 200-fold reduction in N_p (20% RH and 15 ppbv SO_2). A lesser effect for addition of methane compared to propane can be attributed to the difference in their reaction rates with OH.

The dependence of N_p on RH and SO_2 is further demonstrated in the data between 15.8 and 16.3 h and near 17.7 h. RH was decreased from 40% to 10%, and N_p decreased 50-fold (a 98% decrease: actually this decrease is uncertain due to the large uncertainties in the correction factors in measuring an initial N_p of 3.5×10^5 cm^{-3}). When SO_2 was increased from 18 to 30 ppbv, N_p increased about 6-fold. At 17.7 h, SO_2 was decreased to 5 ppbv from 30 ppbv, and N_p decreased about 12-fold.

The finding that SO_2 in the presence of α-particles and water vapor can produce particles has been demonstrated previously.[20−23] The most recent series of papers on this effect[21] show it has a sharp dependence upon [SO_2], water vapor, and residence time. Below ~100 ppbv SO_2, these authors saw very little particle production while we observed significant particle production down to a few ppbv SO_2. Note that the α-source in those studies was about 0.1−0.2 the strength of the one used here; also the residence time in the charger was shorter in the previous work. Nonetheless, it seems prudent to keep this effect in mind for particle monitoring when significant levels of SO_2 are expected to be present in a particle charger. Specifically, residence time within the charging region should be minimized, and if possible, the addition of an appropriate OH scavenger to the sample flow should be considered.

References and Notes

(1) Pandis, S. N.; Russell, L. M.; Seinfeld, J. H. *J. Geophys. Res.* **1994**, *99*, 16945.

(2) McMurry, P. H. *Atmos. Environ.* **2000**, *34*, 1959−1999.

(3) Yu, S.: Kasibhatla, P. S.: Wright, D. L.; Schwartz, S. E.; McGraw, R.; Deng, A. *J. Geophys. Res.* **2003**, *108*, 4353 (doi: 10.1029/2002JD002890).

(4) Kulmala, M.; Vehkamaki, H.; Petaja, T.; Dal Maso, M.; Lauria, A.; Kerminen, V.-M.; Birmili, W.; McMurry, P. H. *J. Aerosol Sci.* **2004**, *35*, 143−176.

(5) Charlson, R. J.; Lovelock, J. E.; Andreae, M. O.; Warren, S. G. *Nature* **1987**, *326* (6114), 655−661.

(6) Bardouki, H.; Berresheim, H.; Vrekoussis, M.; Sciare, J.; Kouvarakis, G.; Oikonomou, K.; Schneider, J.; Mihalopoulos, N. *Atmos. Chem. Phys.* **2003**, *3*, 1871−1886.

(7) Davis, D. D.; Chen, G.; Bandy, A.; Thornton, D.; Eisele, F.; Mauldin, L.; Tanner, D.; Lenschow, D.; Fuelberg, H.; Huebert, B.; Heath, J.; Clarke, A.; Blake, D. *J. Geophys. Res. D* **1999**, *104* (D5), 5765−5784.

(8) Clegg, S. L.; Brimblecombe, P. *Environ. Technol. Lett.* **1985**, *6*, 269.

(9) Kerminen, V.-M.; Leck, C. *J. Geophys. Res. D* **2001**, *106*, 32087 (2000JD900604).

(10) Saltzman, E. S.; Savoie, D. L.; Zika, R. G.; Prospero, J. M. *J. Geophys. Res.* **1983**, *88*, 10897.

(11) Legrand, M.; Sciare, J.; Jourdain, B.; Genthon, C. *J. Geophys. Res. D* **2001**, *106*, 14409.

(12) Huebert, B. J.; Zhuang, L. Z.; Howell, S.; Noone, K.; Noone, B. *J. Geophys. Res.* **1996**, *101*, 4413.

(13) Kido, M.; Osada, K.; Matsunaga, K.; Iwasaka, Y. *J. Geophys. Res. D* **2001**, *106*, 17335.

(14) Van Dingenen, R.; Raes, F. *Aerosol Sci. Technol.* **1991**, *15*, 93.

(15) Jefferson, A.; Eisele, F.; Ziemann, P. J.; Weber, R. J.; Marti, J. J.; McMurry, P. H. *J. Geophys. Res.* **1997**, *102*, 19021.
(16) Poschl, U.; Canagaratna, M.; Jayne, J. T.; Molina, L. T.; Worsnop, D. R.; Kolb, C. E.; Molina, M. J. *J. Phys. Chem.* **1998**, *102*, 10082.
(17) De Bruyn, W.; Shorter, J. A.; Davidovits, P.; Worsnop D. R.; Zahniser, M. S.; Kolb, C. E. *J. Geophys. Res.* **1994**, *99*, 16927.
(18) Schweitzer, F.; Magi, L.; Mirabel, P.; George, C. *J. Phys. Chem. A* **1998**, *102*, 593−600.
(19) Hanson, D. R.; Kosciuch, E. *J. Phys. Chem. A* **2003**, *107*, 2199.
(20) Adachi, M. et al. *J. Aerosol Sci.* **1992**, *23*, 327.
(21) Kim, T. O. et al. *Aerosol Sci. Technol.* **1997**, *26* (6), 527.
(22) Winklmayr, W.; Ramamurthi, M.; Strydom, R.; Hopke, P. K. *Aerosol Sci. Technol.* **1990**, *13*, 394.
(23) Raes, F.; Janssens, J.; Eggermont, G. *Atmos. Environ.* **1985**, *19*, 1069.
(24) Hanson, D.; Orlando, J.; Noziere, B.; Kosciuch E. *Int. J. Mass Spec.* **2004**, *239*, 147.
(25) Viggiano, A. A. et al., *J. Geophys. Res.* **1983**, *87*, 5355.
(26) Schoon, N. et al. *Int. J. Mass Spec.* **2002**, *221*, 209.
(27) Keyser, L. F. *J. Phys. Chem.* **1984**, *88*, 4750−4758, and references therein.
(28) Clegg S. L.; Brimblecombe P.; Wexler, A. S. *J. Phys. Chem. A* **1998**, *102*, 2137−2154 (http://www.uea.ac.uk/∼e770/aim. html).
(29) The activity coefficient of Cl^- was used as a proxy for that of $CH_3SO_3^-$. For RH ≥ 0.5, the effective Henry's law coefficient for MSA is $\geq 10^{11}$ M/ atm, and for typical particle volumes, partitioning to the gas-phase will be 10% or less.
(30) Allen H. C.; Raymond E. A.; Richmond G. L. *J. Phys. Chem. A* **2001**, *105*, 1649.
(31) Baldelli, S.; Schnitzer, C.; Shultz, M. J.; et al. *J Phys Chem B* **1997**, *101*, 10435.
(32) Hanson, D. R.; Eisele, F. *J. Phys. Chem. A* **2000**, *104*, 1715.
(33) Fuchs, N. A.; Sutugin, A. G. *Highly Dispersed Aerosols*; Ann Arbor Science: Ann Arbor, MI, 1970.
(34) Lovejoy, E. R.; Huey, L. G.; Hanson, D. R. *J. Geophys. Res.* **1995**, *100*, 18775.
(35) Hanson, D. R.; Lovejoy, E. R. *J. Phys. Chem.* **1996**, *100*, 6397.
(36) Jayne, J. T.; Duan, S. X.; Davidovits, P.; Worsnop D. R.; Zahniser, M. S.; Kolb, C. E. *J. Phys. Chem.* **1991**, *95*, 6329.
(37) Worsnop, D. W. et al.; *J. Phys. Chem.* **1989**, *93*, 1159. (b) Worsnop, D. W. et al.; *J. Aerosol Sci.* **2001**, *32*, 877−891.
(38) Sugiyama, M.; Koda, S.; Morita, A. *Chem. Phys. Lett.* **2002**, *362*, 56−62.
(39) Morita, A.; Sugiyama, M.; Kameda H.; Koda, S.; Hanson, D. R. *J. Phys. Chem. B* **2004**, *108*, 9111.
(40) Morita, A.; Sugiyama, M.; Koda, S. *J. Phys. Chem. A* **2004**, *108*, 8544−8545.
(41) Hanson, D. R.; Sugiyama, M.; Morita, A. *J. Phys. Chem. A* **2004**, *108*, 3739−3744.
(42) Morita, A. *Chem. Phys. Lett.* **2003**, *375*, 1.
(43) Morita, A.; Sugiyama, M.; Koda, S. *J. Phys. Chem. A* **2003**, *107*, 1749−1759.
(44) Hanson, D. R.; Kosciuch, E. *J. Phys. Chem. A* **2004**, *108*, 8549−8551.
(45) Worsnop, D. R.; Williams, L. R.; Kolb, C. E.; Mozurkewich, M.; Gershenzon, M.; Davidovits, P. *J. Phys. Chem. A* **2004**, *108*, 8542−8543.
(46) Worsnop, D. R.; Williams, L. R.; Kolb, C. E.; Mozurkewich, M.; Gershenzon, M.; Davidovits, P. *J. Phys. Chem. A* **2004**, *108*, 8546−8548.
(47) Noppel, M. *J. Geophys. Res.* **2000**, *105*, 19779−19785.
(48) The density of MSA is 1.48 g/cm^3 while that for sulfuric acid is 1.84 g/ cm^3. *Kirk-Othmer Encyclopedia of Chemical Technology*; John Wiley and Sons: New York, 1983; Vol 22., pp 46 and 190.
(49) Weast, R. C., Ed. In *CRC Handbook of Chemistry and Physics*; CRC Press Inc.: Boca Raton, FL, 1979.
(50) Huthwelker, T.; Peter, T.; Luo, B. P.; Clegg, S. L.; Carslaw, K.; Brimblecombe, P. *J. Atmos. Chem.* **1995**, *21*, 81.
(51) McMurry, P. H.; Friedlander, S. K. *Atmos. Environ.* **1979**, *13*, 1635.
(52) Lovejoy, E. R.; Hanson, D. R.; Huey, L. G. *J. Phys. Chem.* **1996**, *100*, 19911.
(53) Lovejoy, E. R.; Hanson, D. R. *J. Phys. Chem.* **1996**, *100*, 4459.
(54) Nair, P. V. N.; Vohra, K. G. *J. Aerosol Sci.* **1974**, *6*, 265. The Kelvin effect dictates that pH_2O over these small particles is about 2% greater than the bulk[28] pH_2O values. Therefore, the H_2O-content of the particles will be slightly depressed and the values in column 2 in Tables 1 and 2 are a slight underestimate of the H_2SO_4-content of the particles. The underestimate increases with RH: deviation from column 2 value is +0.3 wt % at low RH to +1.6 wt % at RH = 0.9. This also influences the X_{SA} factor in column 6: the calculated decrease in X_{SA} is ∼6% for RH = 0.9. This effect is well within the uncertainties quoted for the surface area of the particles. Finally, this effect upon X_{SA} is expected to mitigate a possible bias due to the assumption of instantaneous drying of the particles within the DMA.